Improving Continuous Hydrologic Modeling of Data-Poor River Basins Using Hydrologic Engineering Center's Hydrologic Modeling System: Case Study of Karkheh River Basin

Rahman Davtalab, Aff.M.ASCE[1]; Ali Mirchi, A.M.ASCE[2]; Sina Khatami[3]; Rabi Gyawali[4]; Alireza Massah[5]; Manuchehr Farajzadeh[6]; and Kaveh Madani, A.M.ASCE[7]

Abstract: This paper applies HEC-HMS to the Karkheh River basin (KRB), Iran, and facilitates the calibration of a continuous hydrologic model (CHM) with soil moisture accounting (SMA) and snowmelt degree-day parameters. Manual calibration was performed to ensure the physical relevance of HEC-HMS parameter values. Because manual calibration entails changing each parameter value in a user-defined setting, it is often a time-consuming procedure complicated by multitude of interacting parameters. To address this setback, an event-based calibration technique (EBCT) was implemented in KRB and its interior sub-basins whereby the governing parameters of specific fall, spring, and winter events were initially estimated in a precalibration step and used as inputs to facilitate calibration of the CHM. Model performance analyzed based on goodness-of-fit criteria with respect to peak flows, low flows, and hydrograph shape reflects uncertainties associated with streamflow naturalization and use of average annual parameter values for the snowmelt component. Sensitivity analysis provided insights into the basin's snowfall and melt characteristics, distinguishing antecedent temperature index (ATI) cold rate coefficient and baseflow recession coefficient as key parameters affecting hydrograph shape and magnitude of the peak flow, respectively. Results based on goodness of fit metrics suggest that event-based parameter estimation using seasonal characteristics improved the efficiency and accuracy of the continuous HEC-HMS model (CORRL and NSE 0.78–0.87 and 0.5–0.7, respectively) while facilitating application to a large, data-poor river basin with heterogeneous climatic conditions. **DOI: 10.1061/(ASCE)HE.1943-5584.0001525.**

Author keywords: HEC-HMS; Event-based calibration technique (EBCT); Snowmelt; Continuous hydrologic model; Calibration; Karkheh River basin.

Introduction

Conceptual water balance models encompass a broad range of hydrologic processes to provide predictive capability for assessing the catchment response to conditions such as land use and climate change (Gyawali and Watkins 2013). Typically, two general approaches are applied in hydrologic modeling, namely event hydrologic modeling (EHM), also known as event-based modeling, and continuous hydrologic modeling (CHM) (Chu and Steinman 2009). The EHM simulates basin response to an individual storm event through a small simulation time window, which may vary from a couple of hours to several days (Gyawali and Watkins 2013). Because runoff in semi-arid areas is typically limited to short periods after storms, EHM is a common approach for modeling such basins (Maneta et al. 2007). In the CHM scheme, a continuous historical record of hydrologic events, including dry and wet spells, is simulated over a number of years (Chu and Steinman 2009). Unlike event-based methods, soil moisture losses including evapotranspiration (ET) and percolation play more significant roles in CHM (Gyawali and Watkins 2013).

Numerous criteria are proposed in the literature to inform hydrologic model selection, which has become a fundamental part of the modeling process because of the availability of several hydrologic models for a specified application. For example, Cunderlik (2003) shortlisted 18 lumped, semidistributed, and distributed models based on four criteria: (1) the quality of model output, (2) proper representation of the required hydrologic processes in the model, (3) the availability of input data, and (4) the modeling cost. In the semidistributed class, Cunderlik (2003) ranked the Hydrologic Engineering Center's Hydrologic Modeling System (HEC-HMS) the highest, above well-known models such as HBV-96, SWAT, and TOPMODEL. HEC-HMS covers a wide range of hydrologic processes, including canopy interception, surface depression, and ground

[1]Graduate Student, Dept. of Civil, Environmental and Construction Engineering, Univ. of Central Florida, Orlando, FL 32816; Dept. of Remote Sensing and GIS, Tarbiat Modares Univ., Tehran, Iran. E-mail: rdavtalab57@gmail.com

[2]Research Assistant Professor, Dept. of Civil Engineering and Center for Environmental Resource Management, Univ. of Texas at El Paso, 500 W University Ave., El Paso, TX 79968 (corresponding author). E-mail: amirchi@utep.edu

[3]Graduate Student, Dept. of Infrastructure Engineering, Univ. of Melbourne, VIC 3010, Australia. E-mail: sina.khatami@unimelb.edu.au

[4]Research Agriculture Engineer, Grazinglands Research Laboratory, Agriculture Research Service, U.S. Dept. of Agriculture, El Reno, OK 73036. E-mail: rabi.gyawali@ars.usda.gov

[5]Associate Professor, Dept. of Irrigation and Drainage Engineering, College of Abureyhan, Univ. of Tehran, Iran. E-mail: armassah@ut.ac.ir

[6]Professor, Dept. of Remote Sensing and GIS, Tarbiat Modares Univ., Tehran, Iran. E-mail: farajzam@modares.ac.ir

[7]Reader, Centre for Environmental Policy, Imperial College London, London SW7 2AZ, U.K.; Dept. of Physical Geography, Stockholm Univ., Stockholm, Sweden. E-mail: k.madani@imperial.ac.uk

Note. This manuscript was submitted on September 25, 2016; approved on January 19, 2017; published online on April 19, 2017. Discussion period open until September 19, 2017; separate discussions must be submitted for individual papers. This paper is part of the ***Journal of Hydrologic Engineering***, © ASCE, ISSN 1084-0699.

water storage, and it accommodates the application of both EHM and CHM approaches (USACE 2010). In this study, HEC-HMS version 3.5 was utilized because it includes a snowmelt component as well as a soil moisture accounting (SMA) algorithm for simulating basin hydrology (USACE 2010). Also, this version supports gridded data sets, facilitating both distributed and semidistributed hydrological modeling. Large river basins can be divided into smaller sub-basins to which different input and parameter sets can be assigned (USACE 2010). Aggregate model inputs (e.g., meteorological data or watershed characteristics) can be provided as spatiotemporal averages as in lumped models (Garcia et al. 2008), facilitating application in settings where high-resolution data are unavailable.

This paper aims to facilitate the application of HEC-HMS models to data-poor river basins with heterogeneous hydroclimatic conditions where calibrating and validating hydrologic models is onerous. In the case of the Karkheh River basin (KRB), challenges in calibrating physically based hydrologic models have motivated the use of statistical models (Zakermoshfegh et al. 2008; Abbasinejad et al. 2014), models with automated calibration capability (Ashraf Vaghefi et al. 2014; Masih et al. 2010; Masih 2011), or simple models with fewer parameters to simulate river flow (Ghanbarpour et al. 2007). As an alternative to the manual calibration approach, automated calibration methods exist within HEC-HMS. However, prior studies have noted the limitations of HEC-HMS's automated calibration module for its inadequacies in the representation of physically relevant parameter estimates (Fleming and Neary 2004; Cunderlik and Simonovic 2004b). The response surface of hydrologic models is often very complex and irregular with numerous local optima (Cunderlik and Simonovic 2004b), making calibration through global optimization very difficult. For this reason, a number of studies (Fleming and Neary 2004; Gyawali and Watkins 2013) have preferred a manual approach to calibration. Further, to model the snow water equivalent (SWE) snow melt algorithm within HEC-HMS requires parameters to be calibrated manually (Cunderlik and Simonovic 2004b). The snow subroutine, added several years after the development of the original model, runs separately, providing results in the form of adjusted precipitation (Fleming and Neary 2004; Gyawali and Watkins 2013; Yilmaz et al. 2012). Using the KRB as a case study, this paper presents procedures to facilitate the manual calibration of HEC-HMS CHM, including the parameters of the SMA model and snowmelt degree-day method.

Study Area: Karkheh River Basin

The KRB (Fig. 1) is an important transboundary river basin whose environmental and economic significance, as well as future food security and hydropower production challenges, have been recognized nationally and internationally (Ashraf Vaghefi et al. 2014; Ahmad and Giordano 2010). It is mostly semi-arid with an average precipitation of 450 mm/year and average evaporation of 2,200 mm/year (IRME 2012). The basin is dry and warm in the south, close to the Persian Gulf, with less than 200 mm/year precipitation. In the northern mountainous part, however, it receives more than 800 mm/year precipitation, of which 60% is snow (Saghafian and Davtalab 2007). With an area of more than 50,000 km^2, the KRB is Iran's third largest river basin in terms of potential for hydropower generation (Jamali et al. 2013). The basin is shared by seven provinces, five of which—namely Kermanshah, Hamedan, Ilam, Lorestan, and Khouzestan [Fig. 1(a)]—supply water to more than 4 million people. Iran's largest reservoir [> 5 billion cubic meters (BCM)] formed by the Karkheh Dam is located in the south central part of the basin,

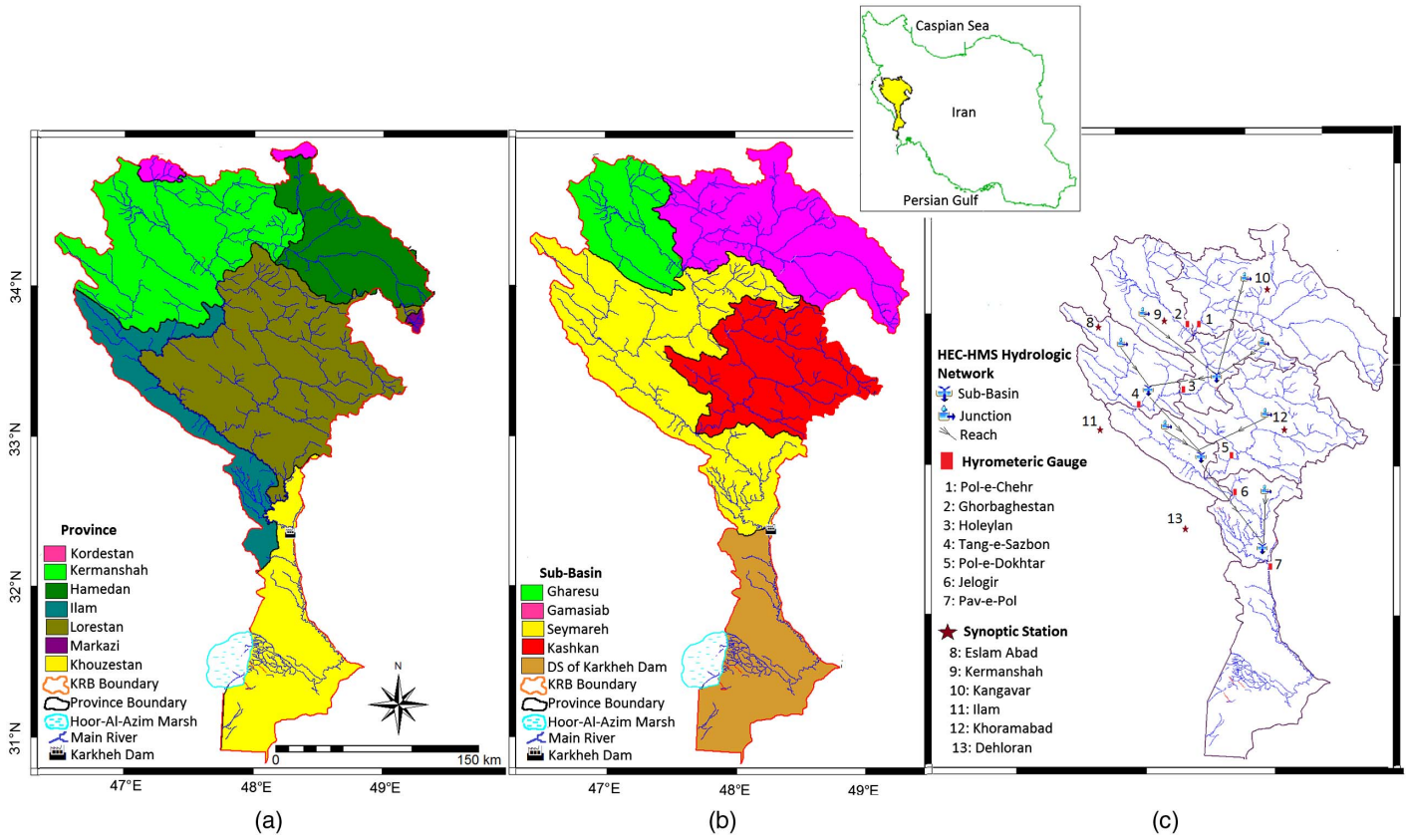

Fig. 1. KRB with its (a) provincial divisions; (b) sub-basins; (c) selected hydrometric and synoptic stations and conceptual HEC-HMS model

Table 1. Representative Synoptic Stations for Each Sub-Basin

Station	Latitude (degrees)	Longitude (degrees)	Altitude (m)	Data available from	Area covered
Kangavar	34.50	47.98	1,468	1987	Gamasiab
Kermanshah	34.35	47.15	1,319	1961	Gharesu and lateral basin until Holeylan station
Eslamabad	34.12	46.47	1,349	1987	Lateral basin until Tang-e-Sazbon station
Ilam	33.63	46.43	1,337	1982	Lateral basin
Khoramabad	33.43	48.28	1,147	1961	Kashkan
Dehloran	32.68	47.27	232	1987	Lateral basin from Karkheh Dam up to Jelogir station

Table 2. Hydroclimatic Conditions Upstream of Each Hydrometric Gauge

Sub-basin	Hydrometric station	Area (km^2)	Observed annual runoff (mm/year)	Naturalized annual runoff (mm/year)	Temperature			Precipitation (mm/year)	Evaporation (mm/year)
					Maximum (°C)	Mean (°C)	Minimum (°C)		
Gharesu	Ghurbaghestan	5,370	135	181	20.5	12.2	4.3	504	1,947
Gamasiab	Pol-e-Chehr	10,860	100	120	19	10.9	3	489	1,973
Lateral	Holeylan	20,863	118	151	19.6	11.5	3.5	503	1,961
Seymareh	Tang-e-Sazbon	25,976	116	156	20	12.0	3.9	506	1,977
Kashkan	Pol-e-Dokhtar	9,140	184	197	21.3	13.8	5.7	566	2,053
Lateral	Jelogir	39,940	126	151	20.5	12.6	4.5	510	2,006
Karkheh Dam	Pay-e-Pol	42,620	140	160	21.3	13.5	5.5	510	2,074

receiving water from the four upstream sub-basins of Gharesu, Gamasiab, Seymareh, and Kaskan (Fig. 1). The major water use sectors include agricultural lands, urban areas, and fish farms (IRME 2012). The Karkheh River also supplies water to Hoor-Al-Azim international wetland, which is drying up because of severe droughts and increasing development in Iran and Iraq (Ashraf Vaghefi et al. 2014).

Six representative synoptic stations [Fig. 1(c) and Table 1] record daily and hourly temperature, precipitation, type of rainfall, and evaporation (class A pan). River flow in the KRB's three main sub-basins, i.e., Gamasiab, Gharesu, and Kashkan, is measured at Pol-e-Chehr, Ghorbaghestan, and Pol-e-Dokhtar stations, respectively. Four other stations provide cumulative river flow at the confluence of rivers upstream of the Karkheh Dam. Table 2 summarizes the general hydroclimatic conditions upstream of each hydrometric station. The basin elevation varies from less than 150 m above sea level to more than 3,600 m. The basin area upstream of Karkheh Dam (i.e., at Pay-e-Pol station) is approximately 43,000 km^2 with an average annual flow volume of approximately 6 BCM.

Average precipitation, temperature, and evaporation (class A pan) are listed in Table 2. Isohyetal and isothermal maps were prepared using elevation gradient and the digital elevation model (DEM). The isolines were corrected by error maps extracted from the difference between observed and calculated values at the stations (IRME 2012). Results reflect a wide variation in precipitation gradient (e.g., 200 mm to more than 1,000 mm per 1,000 m altitude increment). Thermal gradient has less variation, changing from −6 to −7°C per 1,000 m altitude increment, which agrees with values given by Martinec (1975). Because of low precipitation and high evaporation in the lower basin, natural surface water availability downstream of the Karkheh Dam is negligible. Therefore, the model was calibrated only for areas located upstream of the dam [Fig. 1(c)].

HEC-HMS Model

The HEC-HMS modeling system includes three components: (1) river basin model, (2) meteorological model, and (3) control specifications. Each component is discussed subsequently, including the snow melt algorithm within the meteorological model.

River Basin Model

The HEC-HMS basin model simulates the water cycle, from canopy to soil surface and groundwater, excluding deep groundwater. SMA, a loss algorithm used in the CHM of the HEC-HMS (Leavesley et al. 1983), takes precipitation and ET as inputs and computes surface runoff, groundwater flow, and losses due to ET and deep percolation [Fig. 2(a); see USACE (2000) for detailed explanation]. Clark Unit Hydrograph was selected for the transform method (or simulating hydrograph), Muskingum for routing, and the recession method for baseflow calculation (Viessman and Lewi 1995; USACE 2000). Initial parameters for the Clark method were estimated using land cover, soil texture, and physiographic data. The K value for the Muskingum method was estimated based on flow velocity and reach length of the gauged basin. The average value of 0.3 was used as a starting X value. The initial K and X had small changes during the calibration, and all X values were in the range of 0–0.5 (USACE 2000). Physiographic parameters (e.g., river length, drainage area, slope, etc.) of the sub-basins at the outlet of the seven selected hydrometric stations [Fig. 1(c)] were calculated in geographic information systems (GISs) using 1:250,000 topographic maps (Iran National Cartographic Center: http://www.ncc.org.ir) with 100-meter contours (Table 3). The 1:250,000 resolution of topographic maps was deemed adequate for parameter calibration (Croley et al. 2005). The parameters of the recession constant and peak ratio for baseflow were estimated during calibration.

The basin model includes 24 parameters, 18 of which belong to the SMA model, and the rest of which are used for simulating routing, baseflow, and hydrograph. Previous studies (e.g., Fortin et al. 2001; Fleming and Neary 2004; Neary et al. 2004; Yilmaz et al. 2012; Gyawali and Watkins 2013; Khatami and Khazaei 2014) have used the following methods for parameter estimation: (1) utilizing geodatabases, (2) reducing the number of free parameters by initializing the simulation in periods when the initial conditions are easier to assume or estimate (in this case, the beginning of fall or September 22, which marks the beginning of the water year in Iran), and (3) using empirical equations or credible sources. A combination of these three methods was applied. Soil texture information (Table 4) was extracted from an existing interpolated soil

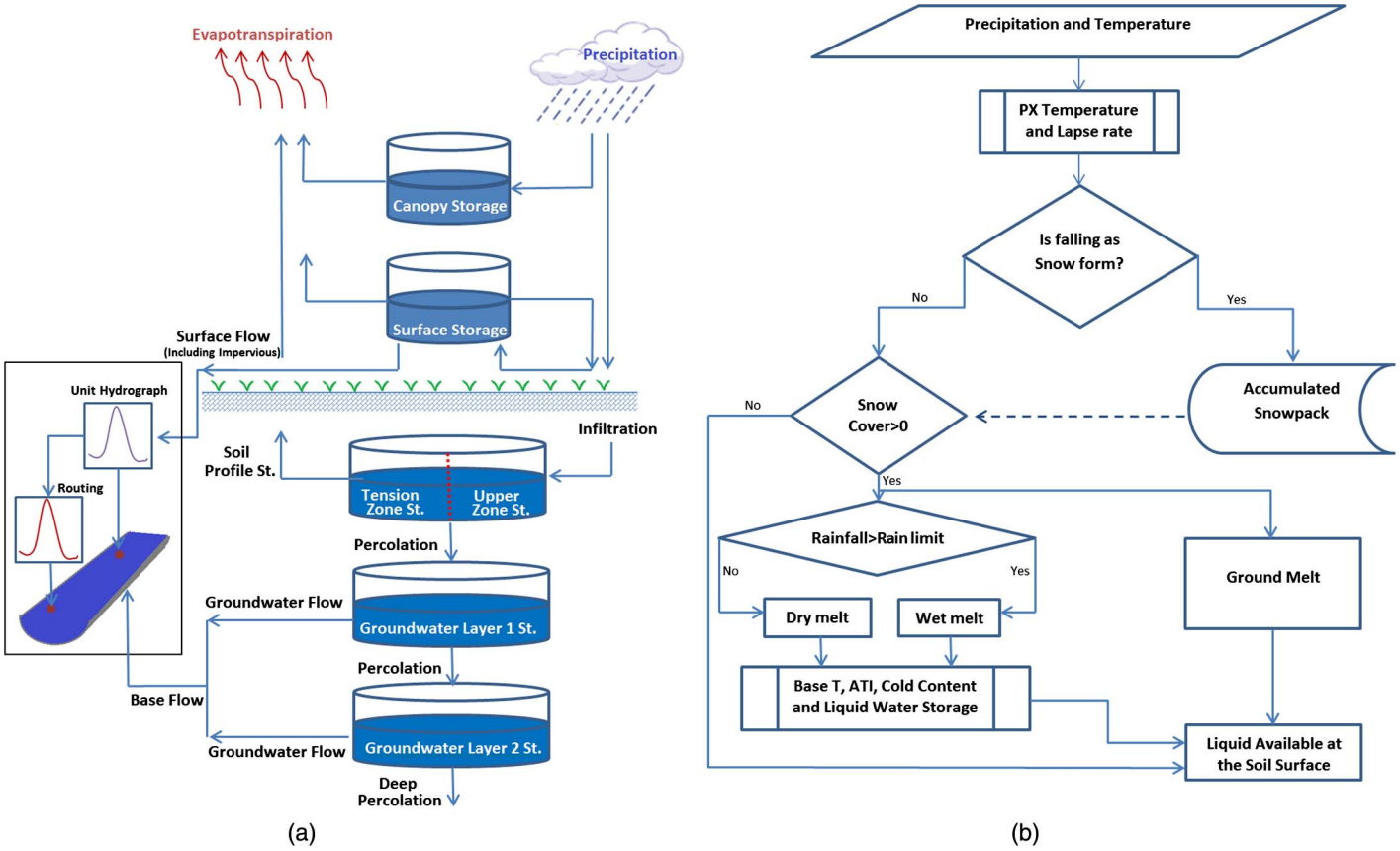

Fig. 2. (a) Schematic of basin model in HEC-HMS and its principal components; (b) flowchart of snowmelt model (adapted from USACE 2000; Gyawali and Watkins 2013)

Table 3. Physiographic Parameters Upstream of the Hydrometric Gauges

Hydrometric station	Area (km^2)	River length (km)	Maximum altitude (m)	Mean altitude (m)	Minimum altitude (m)	Mean slope (%)
Ghurbaghestan	5,370	204	3,300	1,575	1,300	12
Pol-e-Chehr	10,860	255	3,600	1,890	1,300	15
Holeylan	20,863	381	3,600	1,772	1,000	15
Tang-e-Sazbon	25,976	449	3,600	1,708	800	15
Pol-e-Dokhtar	9,140	294	3,600	1,647	700	20
Jelogir	39,940	606	3,300	1,640	400	17
Pay-e-Pol	42,620	765	3,600	1,568	150	17

texture class map of Iran produced based on more than 4,000 soil profile data points (Hengl et al. 2007). Canopy maximum interception and soil surface storage were estimated by vegetation type and slope percentage, respectively (Fleming and Neary 2004; Bennett 1998). The infiltration rate and percolation in the soil profile and groundwater were estimated based on hydraulic conductivity (Fleming and Neary 2004). Saturated point, field capacity, wilting point, and hydraulic conductivity were calculated based on a method proposed by Saxton et al. (1986) using an online tool (http://staffweb.wilkes.edu/brian.oram/?soilwatr.htm) that takes percentages of sand and clay as inputs. The depth of active soil was assumed to be 60 cm based on the cropping pattern (IWRM 2009) and land cover. Fleming and Neary (2004) estimated the HEC-HMS groundwater storage (i.e., groundwater 1 and groundwater 2) and percolation parameters (USACE 2010) based on recession analysis. These estimates were used as initial values for calibration and were adjusted during the process.

Meteorological Model

Temperature, precipitation, and ET are inputs to the meteorological model. The synoptic stations are located in the middle elevation of the sub-basin, representing the average precipitation condition.

Table 4. Soil Properties of the Sub-Basins

Hydrometric station	Sand (%)	Clay (%)	Wilting point (mm)	Field capacity (mm)	Saturation (mm)	Saturated hydraulic conductivity (mm/h)	Available water (mm)	Soil storage (mm)	Upper zone (mm)	Tension storage (mm)
Gharesu	53	47	150.4	203.3	304.2	1.1	52.8	153.7	100.9	52.8
Gamasyab	50	35	116.8	179.1	295.7	2.0	62.3	178.8	116.6	62.3
Holeylan	36	51	169.0	237.2	314.3	1.3	68.3	145.3	77.0	68.3
Tang-e-Sazb	47	49	158.1	215.8	308.2	1.1	57.7	150.0	92.3	57.7
Kashkan	36	51	169.0	237.2	314.3	1.3	68.3	145.3	77.0	68.3
Jelogir	31	51	171.2	245.0	316.4	1.5	73.8	145.2	71.4	73.8
Pay-e-Pol	39	34	113.6	188.7	299.5	2.6	75.0	185.9	110.8	75.0

Likewise, daily temperature data, maximum and minimum temperature, relative humidity, wind speed, and sunshine hours were obtained at the sub-basin scale. HEC-HMS extrapolates the observed temperature pertaining to different elevations using the lapse rate value. The model allows division of each sub-basin into different elevation bands with unique boundary conditions. Elevation bands of 200-m intervals were used based on the resolution of DEM. Based on the mean annual lapse rate and snowmelt component, precipitation may fall as snow or rain [Fig. 2(b)]. The snowmelt procedure is separately applied on the accumulated snowpack for each elevation boundary. For estimating ET, a FAO-Penman-Monteith equation (FAO 2004) was chosen, as in *CROPWAT version 8*. The required data (wind speed, sunshine, relative humidity, and temperature) were acquired from the synoptic stations.

The snowmelt component is an important part of the meteorological model, especially for mountainous areas of the upper KRB, where snowpack significantly affects river flow regime by storing water during the fall and winter seasons and releasing it during the melt season. Snowmelt is typically estimated using two methods: (1) the energy balance method, using the heat balance equation, and (2) the temperature-index (TI), which uses a linear relationship between air temperature and snowmelt rate (Hock 2003). Although the energy balance method better represents the melt processes, it is computationally intensive and requires variables that are largely unavailable for the KRB. For its simplicity, the TI is widely used in hydrologic models (Martinec 1960; Leavesley 1989; Hock 2003), including HEC-HMS. Overall, the TI is recognized as a practical snowmelt model for the KRB (Omani et al. 2007; Fuladipanah and Jorabloo 2012; Solaymani and Gosian 2012) because of its simplicity, parsimonious data requirements, and its generally "good" performance as compared with physically based energy balance models (Hock 2003; Morid et al 2004; Zeinivand and De Smedt 2009). A small amount of snowfall may occur in temperatures above 5°C, and a small amount of rainfall below 0°C has been observed (Fig. 3). The temperature of 50% snowfall was chosen as the initial criterion for the snowfall threshold temperature (i.e., PX temperature) in the KRB (Saghafian et al. 2016). The initial value of 2.74 mm/°C/day was chosen for its degree-day factor (DDF) based on previous recommendations (USDA 2004).

The antecedent temperature index (ATI) melt rate was applied such that weather conditions (based on mean daily temperature) affecting the current melt rate were represented. Eq. (1) shows the effect of ATI on snowmelt (Ferner and Wigham 1985). KRB, located at low latitudes, has an ephemeral snow cover. Typically, a constant melt rate is considered for such regions along with a monthly adjustment factor (Gyawali and Watkins 2013)

$$M_{td} = \mathrm{DMR} \times [T_{td} - T_b + K(\mathrm{ATI}_{td-1})] \times \mathrm{SAF}_m \qquad (1)$$

where M_{td} = amount of snowmelt for today (mm); DMR = dry melt rate (mm/°C/day); T_{td} = mean daily air temperature for today (°C); T_b = base temperature (°C); ATI_{td-1} = ATI value for yesterday (°C); K = ATI coefficient; SAF_m = monthly adjustment factor; and $[T_{td} - T_b + K(\mathrm{ATI}_{td-1})]$ = ATI value for today (°C). The base temperature is the same as the freezing temperature (typically 0).

The ATI cold rate coefficient, ATI cold rate function, and cold limit in the snowmelt algorithm determine the amount of heat needed to increase the snowpack temperature to 0°C (i.e., cold content). The amount of liquid water held in the snowpack was set to 4% in the model and a constant value of 0.2 mm/day was applied to account for snow melted by ground heat (USACE 2010).

Flow Naturalization

Because of anthropogenic modifications of the KRB during the past century, the observed river flows at the hydrometric stations do not reflect the unimpaired or natural hydrologic response of the basin (Table 2). Therefore, there are significant uncertainties associated with the observed flow data that cannot simply be expressed in statistical terms (Beven 2016) and could be a potential source of "disinformation" (Beven and Westerberg 2011). Flow naturalization (or estimating the virgin flow) is defined as removing the effects of upstream flow regulations (including evaporation from reservoir), water withdrawals, and return flows (Wurbs 2006). Almost all the water withdrawal in this part of the basin is through pumping and diverting water to irrigation furrows or canals (IWRM 2009). Because there is no operational reservoir upstream of the Karkheh Dam, flow naturalization was done by adjusting agricultural water withdrawals and associated return flows.

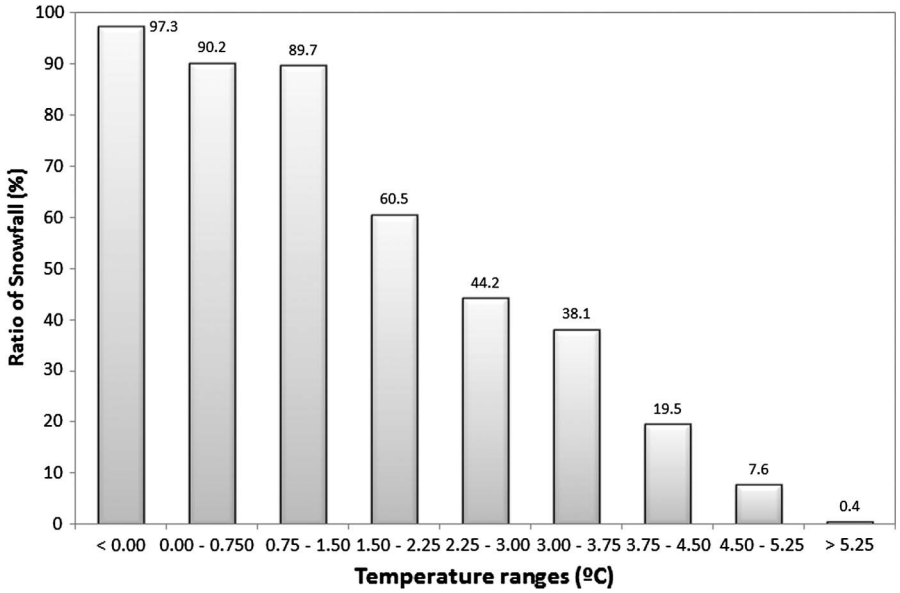

Fig. 3. Percentage of snowfall in different ranges of daily temperature

Ideally, naturalized flows (i.e., unimpaired flow) can be obtained by adding the difference between measured withdrawals and return flows to the observed flow at hydrometric stations (Naik and Jay 2005; Wurbs 2006). A tool called NETWAT (IRMJA and IRMO 1999) was used, which was specifically developed to calculate the net irrigation water needs of more than 600 agricultural plains of Iran using a meteorological data bank. NETWAT selects a representative synoptic station and estimates the net irrigation water needs using the following equation (IRMJA and IRMO 1999):

$$\text{Irnet}_n = ET_0 \times Kc_n - P_e \tag{2}$$

where Irnet_n = irrigation water need for crop n (mm/day); ET_0 = reference potential evapotranspiration (mm/day); Kc_n = crop coefficient for crop n; and P_e = effective rainfall (mm/day).

NETWAT uses FAO-Penman-Monteith to calculate ET_0 (FAO 1986). Total withdrawal from surface water is calculated using Eq. (3)

$$W_s = 10 \times \frac{\sum \text{Irnet}_n \cdot A_n}{e} \tag{3}$$

where W_s = surface water withdrawal (m^3/day); A_n = cultivated area of crop n (ha); and e = irrigation efficiency.

Naturalized river flow for each station is calculated using Eq. (4)

$$F_N = F_O + W_s - \alpha \times W_s \tag{4}$$

where F_N = naturalized flow for each station (m^3/day); F_O = observed flow (m^3/day); and α = coefficient of surface returned flow.

Because of the unavailability of measured data on water withdrawal and return flow, these values were estimated based on cropping pattern, irrigation water need, cultivated area, and irrigation efficiency (Masih 2011). Average surface water irrigation efficiency in the KRB is approximately 30% (IRME 2012). Irrigation return flow is approximately 20–30%, and runoff is twice as large as infiltration volume (Pirmoradian et al. 2004). Therefore, the value of 0.15 was assumed for the coefficient of the surface return flow. Fig. 4 shows observed and naturalized flows at the Pay-e-Pol hydrometric station.

Calibration and Validation Strategy

Manual parameter calibration begins with an educated estimate of initial parameters to run the model. The KRB model was developed at daily time scale using a 14-year simulation horizon (1987–2000) split between calibration (1994–2000) and validation (1987–1994) periods. Because the basin's summer precipitation is negligible (Alijani 1995), the simulation can be initiated at the beginning of the fall (i.e., September 23) when the soil is almost dry. As such, the initial storages of canopy, surface, soil profile, and groundwater 1 and 2 were safely assumed negligible, eliminating these five parameters. These initial storages affect the simulated hydrograph from a couple of days to a maximum of several months (McEnroe 2010) but they are insignificant from the perspective of long-term water resource planning. Subsequently, simulated results are compared with observed data using a set of performance criteria. Depending on which submodel is selected, the CHM method of the HEC-HMS may include 25 to 40 calibration parameters, making manual calibration an onerous procedure.

Event-Based Calibration Technique

Despite the advantages of the systematic calibration approach, the calibration process has typically remained tedious and time consuming because of the large number of interacting parameters. To address this challenge, an event-based calibration technique (EBCT) (Fig. 6) was applied to improve the calibration time and simulation accuracy by reducing hydrologic complexity (Fleming and Neary 2004; Cunderlik and Simonovic 2004b). In essence, the EBCT facilitates systematic calibration of the HEC-HMS when applied to large, data-poor regions with varied hydroclimatic conditions such as the KRB. As a part of the EBCT, hydrologic events were classified based on their characteristics. A precalibration sensitivity test was conducted to identify the governing hydrological or meteorological parameters and to reduce the number of calibration parameters. The key parameters identified were sequentially changed one at a time while keeping other parameters constant or excluding them altogether. The initial parameter value was incrementally decreased or increased by 10% within a range of ±75% as a soft

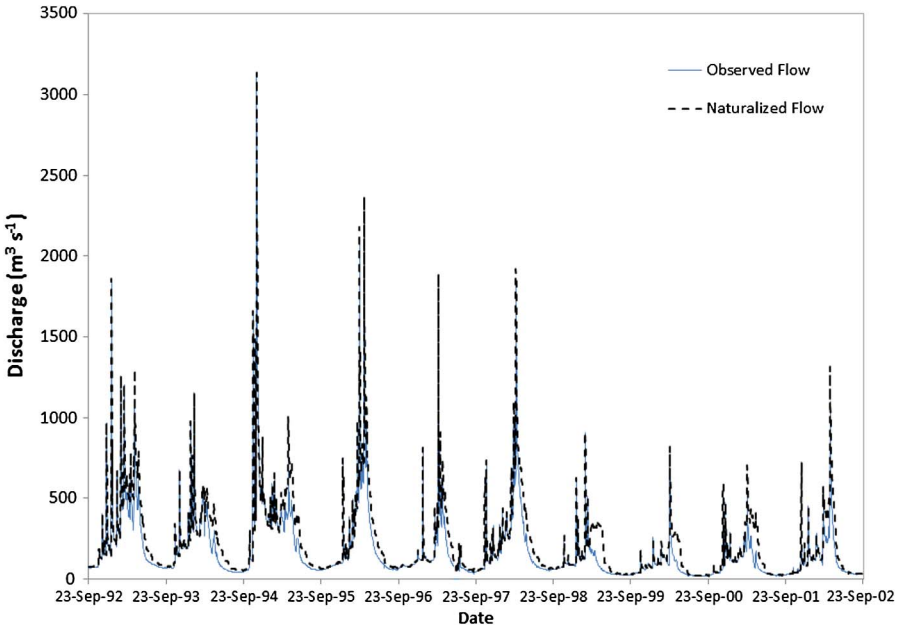

Fig. 4. Naturalized river flow and observed flow at Pay-e-Pol hydrometric station

limit, which typically provides reasonable parameter estimates (Cunderlik and Simonovic 2004b).

Hydrologic events were classified into three different clusters, i.e., early fall, spring, and winter events (Fig. 5), to estimate initial parameter values and eventually improve the final all-inclusive model calibration process. The early fall events in the KRB have two major differences from the winter and spring events. In the fall, there is negligible to no snowfall in the basin, and there is no snowpack because of the prior warm summer. Therefore, for the early fall events, the snowmelt model parameters were excluded from the hydrologic process. The early fall events were further divided into three subclusters, including events with durations less than the time of concentration (Tc), other single peak events, and multiple peak events. When calibrating the model to capture the events with durations less than the time of concentration, emphasis was placed on tuning the top soil parameters such as canopy storage, soil surface storage, and maximum infiltration rate. For other single peak events, the soil storage, tension storage, and soil percolation were calibrated, whereas for the multiple peak events, the parameters related to groundwater 1 and groundwater 2 were considered. Unlike fall events, the snowmelt model was the predominant hydrologic process for spring, including snowmelt caused by warm rainfall. Rainfall or snowfall on snowpack or on ground constitute major events in winter and late fall and therefore all snow melt parameters affected the basin response to the precipitation events.

As an example of an event classification, the hydrograph of November 1994 formed by an intense early fall rainfall (approximately 100 mm in 48 h) is shown in Fig. 6. During this event, groundwaters 1 and 2 do not play a perceptible role in the rainfall-runoff process. In other words, because of the insensitivity of the hydrograph shape or the runoff volume to these parameters, the hydrograph is deemed suitable for calibrating the upper soil layer parameters.

Splitting the data to conduct calibration and validation runs is an important but subjective hydrologic modeling decision and is often project dependent (e.g., Yilmaz et al. 2012; Gyawali and Watkins 2013; Fleming and Neary 2004). To select suitable individual rainfall-runoff events for calibration and validation of the HEC-HMS, Cunderlik and Simonovic (2004a) considered three criteria: (1) long sequences of concurrent precipitation, temperature, and streamflow records; (2) representative hydrologic variability in terms of mean and extremes in the selected sequences; and (3) the most possible spatiotemporal density of data records (i.e., precipitation, temperature, and streamflow). Based on these criteria, the period of 1994–2000 was selected for calibration. This period includes a fall season flood hydrograph (rainfall with antecedent dry soil), snowmelt (due to heat waves or warm spring rainfall), drought periods, and extreme flooding. The model performance was then evaluated using the period of 1987–1994, which includes wet, dry, and average climate conditions.

Several fitness factors can be used to evaluate model performance (i.e., predictive power). Some factors focus on extreme values (peak or low flows), whereas others focus on hydrograph shape or runoff volumes. The fitness factors used include ratio of simulated to observed runoff volume (RSORV), average of error in peak flow (AEPF), average error in low flow (AELF), Nash-Sutcliffe model efficiency (NSE), and coefficient and linear correlation coefficient (CORRL) (Gyawali and Watkins 2013). AELF is not applicable to arid areas with low flow value of zero

$$\text{AEPF} = 100 \times \left(\sum_{i=1}^{N} |\text{QPO}_i - \text{QPS}_i| / \text{QPO}_i \right) \Big/ N \quad (5)$$

$$\text{AELF} = 100 \times \left(\sum_{i=1}^{N} |\text{QLO}_i - \text{QLS}_i| / \text{QLO}_i \right) \Big/ N \quad (6)$$

$$\text{NSE} = 1 - \sum_{i=1}^{N} (QO_i - QS_i)^2 \Big/ \sum_{i=1}^{N} (QO_i - QO_m)^2 \quad (7)$$

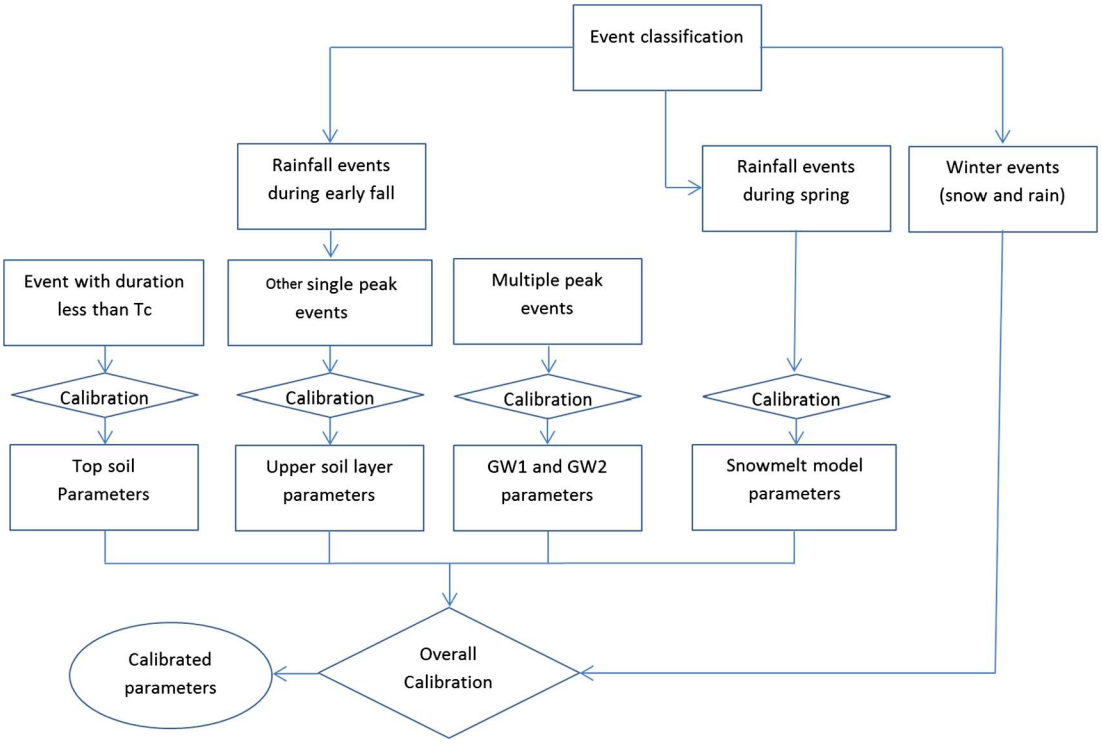

Fig. 5. Event classification and major steps of EBCT (Tc: time of concentration)

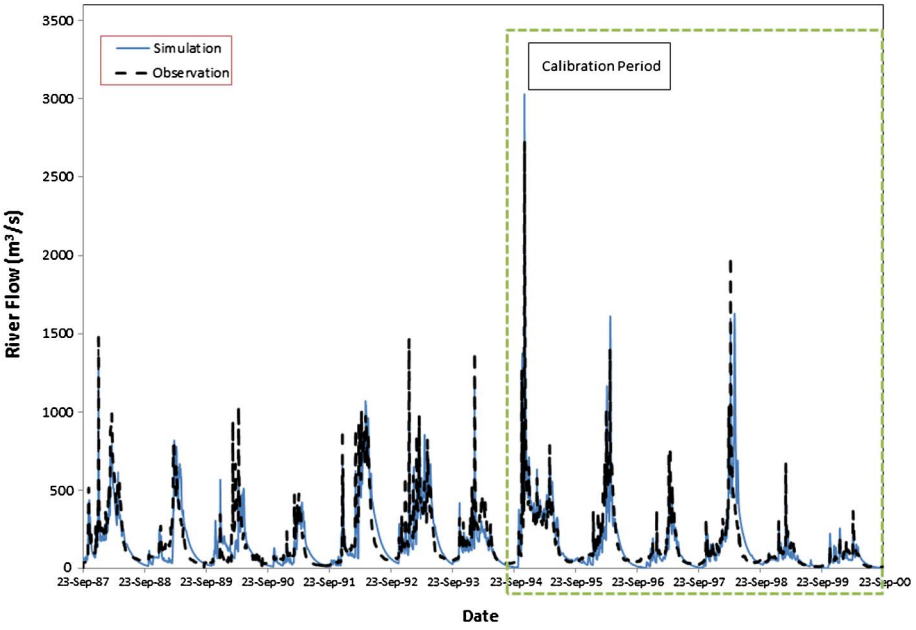

Fig. 6. Comparison of daily simulated and observed hydrograph at Jelogir station

$$\text{CORRL:}\frac{\sum_{i=1}^{N}(QO_i - QO_m)\times(QS_i - QS_m)}{\sqrt{\sum_{i=1}^{N}(QO_i - QO_m)^2 \times \sum_{i=1}^{N}(QS_i - QS_m)^2}} \quad (8)$$

where QO = observed flow; QS = simulated flow; QPO = observed peak flow for each hydrograph; QPS = simulated peak flow for each hydrograph; QLO = observed low flow for each hydrograph; QLS = simulated low flow for each hydrograph; QO_m = mean observed flow for the appropriate period; and N = number of computed hydrograph ordinates. The unit for all flow values is m^3/s. AEPF and AELF are percentages, whereas RSORV, NSE, and CORRL are unitless.

Sensitivity Analysis

Sensitivity analysis is useful in different phases of the modeling process, namely model formulation, calibration, and validation (McCuen 1973). Various sensitivity analysis techniques help avoid overparameterization, which is ubiquitous in hydrologic modeling, especially in distributed models (Van Griensven et al. 2006). A local sensitivity analysis method (Haan 2002) was applied using Eq. (10)

$$SA = \frac{\partial O}{\partial P} \quad (10)$$

where SA = absolute sensitivity coefficient; O = model output; and P = particular parameter (Cunderlik and Simonovic 2004b).

The local method is simpler as compared with the global sensitivity analysis method, which uses random parameter changes. Three dimensionless fitness factors were employed to compare the parameter sensitivities, including relative root mean square error (RRMSE), percent of error in peak (PEP), percent of error in volume (PEV), and linear correlation coefficient (Cunderlik and Simonovic 2004b)

$$\text{RRMSE} = 100 \times \sqrt{\frac{1}{N}\sum_{i}^{N}\left(\frac{QO_i - QS_i}{QO_i}\right)^2} \quad (11)$$

$$\text{PEP} = 100\times\left|\frac{QP_o - QP_s}{QP_o}\right| \quad (12)$$

$$\text{PEV} = 100\times\left|\frac{V_o - V_s}{V_o}\right| \quad (13)$$

where V_o = observed volume (MCM); and V_s = simulated volume (MCM).

To perform the sensitivity analysis, the final set of calibrated parameters was used to generate the baseline hydrograph. Subsequently, the model was rerun by changing a particular parameter by ±20% (Cunderlik and Simonovic 2004b), and the new hydrographs were compared with the baseline hydrograph using the previous relative fitness factors.

Results

Calibrated model parameters for the three main sub-basins of the KRB, namely Gamasiab, Gharesu, and Kashkan, are summarized in Table 5. Daily hydrographs for calibration and validation periods at Jelogir station are shown in Fig. 6, and the goodness-of-fit values are summarized in Table 6. All correlation coefficients are significant at 1% confidence interval, and NSE has acceptable values for all sub-basins (Table 6). Jelogir station has the best CORRL and NSE fitness factors, denoting that at this station the calibrated parameters can best represent the average conditions of the basin.

Acceptable RSORV values (i.e., close to 1) indicate the calibrated model's ability to estimate runoff volume (Table 6), which is the governing component of water availability in this basin and thus a critical input for water budget analysis and water allocation. Overall, the runoff volume estimates were better than peak and low flow estimates as indicated by superior RSORV values as compared to AEPF and AELF. Based on AEPF and AELF and visual assessment of the hydrographs, the model simulates peak flows better than low flows, in part because of the uncertainty of river flow naturalization. In addition, large withdrawals and low precipitation during summer and at the end of spring result in low river flow.

Table 5. Calibrated Parameters for Three Main Sub-Basins of the KRB

Sub-models	Parameter	Abbreviation	Gamasiab	Gharesu	Kashkan
Canopy method	max (mm)	Cs	1.2	1.5	1.5
Surface method	max (mm)	Ss	30	18	20
Loss method	Max infiltration rate (mm/h)	In	10	1.5	6
	Impervious (%)	Im	8	9	10
	Soil storage (mm)	Sst	20	10	50
	Tension storage (mm)	Ts	8	4	20
	Soil percolation (mm/h)	Sp	20	5	30
	GW1 storage (mm)	Gs1	70	100	40
	GW1 percolation (mm/h)	Gp1	8	4	0.05
	GW1 coefficient (h)	Gc1	500	2000	500
	GW2 storage (mm)	Gs2	10	40	2
	GW2 percolation (mm/h)	Gp2	0.02	0.05	1
	GW2 coefficient (h)	Gc2	500	2000	600
Transform	Time of concentration (h)	Ts	51	47	50
	Storage coefficient (h)	Tc	75	95	55
Base flow	Recession constant	Bc	0.97	0.97	0.98
	Ratio	Bra	0.25	0.25	0.11
Snowmelt	PX temperature (°C)	PXT	1.5		
	Wet melt rate (mm/ deg -day)	WMR	4		
	ATI melt rate coefficient	ATIMC	0.75		
	ATI melt rate function	DMR	2.5 (fixed)		
	ATI cold rate coefficient	ATICC	0.7		

Table 6. Model Performance in Terms of Goodness-of-Fit Indices for the Calibration and Validation Periods

			RSORV		AEPF (%)		AELF (%)		NSE		CORRL	
Sub-basin	Station	Area (km^2)	Cal.	Val.	Cal.	Val.	Cal.	Val.	Cal.	Val.	Cal.	Val.
Gharesu	Ghurbaghestan	5,370	1.20	1.17	31.7	25.3	31.7	51.0	0.52	0.57	0.86	0.74
Gamasiab	Pol-e-Chehr	10,860	1.02	0.93	12.4	20.4	21.2	30.0	0.54	0.38	0.79	0.75
Lateral1	Holeylan	20,863	1.04	1.07	20.9	10.0	25.0	30.0	0.62	0.49	0.86	0.81
Seymareh	Tang-e-Sazbon	25,976	0.89	0.95	22.9	14.9	17.0	23.8	0.50	0.47	0.78	0.85
Kashkan	Pol-e-Dokhtar	9,140	1.14	1.05	33.7	23.7	54.4	63.0	0.57	0.49	0.79	0.76
Lateral2	Jelogir	39,940	1.02	0.98	18.9	11.0	21.8	25.2	0.70	0.76	0.87	0.88
Karkheh Dam	Pay-e-Pol	42,620	1.06	0.98	12.1	15.9	21.7	27.3	0.60	0.70	0.81	0.81

The use of average basin scale snow parameters (especially DDF and ATI-coldrate and wetrate coefficients) does not accommodate sub-basin–scale snow parameter inputs, affecting the model performance in large, hydroclimatically varied basins of the KRB. In particular, model performance in snow-dominated headwater sub-basins of the KRB (e.g., Gharesu and Kashkan) was adversely affected because of this limitation.

Furthermore, the results of the average flow conditions were found to be superior to the results for extreme conditions. In extremes, the model reproduced wet periods better than dry periods. Relatively poor model performance under drought conditions may be attributed to uncertainty associated with the flow naturalization process. During severe drought periods, the regional cropping pattern is changed as an adaptation strategy. However, these extreme event adaptations (e.g., cultivated crops and associated cultivation area) are poorly documented, creating a source of uncertainty.

The classic split-sample conditional validation (Klemeš 1986) was carried out to evaluate the calibration results, i.e., no parameter was changed throughout the validation process. The validation results better represent the model's predictive power (Gyawali and Watkins 2013), potentially due to overfitting the model to the observed data during the calibration. Conditional validation confirmed that the model was adequately calibrated (Table 6 and Fig. 6), although in some sub-basins, the validation results were somewhat better than the calibration results.

Fig. 7 illustrates the sensitivity of 17 parameters of HEC-HMS at the Pay-e-Pol hydrometric gauge (upstream of the Karkheh Dam) as an example, based on different goodness-of-fit metrics.

The DDF (including WMR and DMR) and ATICC are the most sensitive parameters, as indicated by the CORRL factor (an indicator of hydrograph shape) [Fig. 7(a)]. A high CORRL factor is obtained when two sets of flow time series have similar variability pattern. Therefore, the timing of fluctuation pulses is more important than the magnitude of maximum and minimum parameter values in absolute terms. Changing the snow melt parameters introduces a significant lag time for runoff time series by increasing or decreasing the snowpack or snowmelt runoff. The model is most sensitive to DDF when the parameter values are decreased up to 20% [Fig. 7(a)]. When the parameter values are increased by 20%, however, ATICC becomes the most sensitive parameter. This is because the amount of snowpack in the basin is limited; thus, increasing the DDF does not continue to change runoff volume significantly after the snow melts completely. On the other hand, decreasing this value can store a large amount of water in the basin as snowpack. Increasing ATICC has the opposite effect by saving more cold energy and hence a larger snowpack volume. The baseflow recession constant (Bc) was found to be the most sensitive parameter. Changing Bc by 20% resulted in a more than 35% change of RRMSE [Fig. 7(b)]. The peak flow and runoff volume errors (PEP and PEV) are most sensitive to groundwater parameters

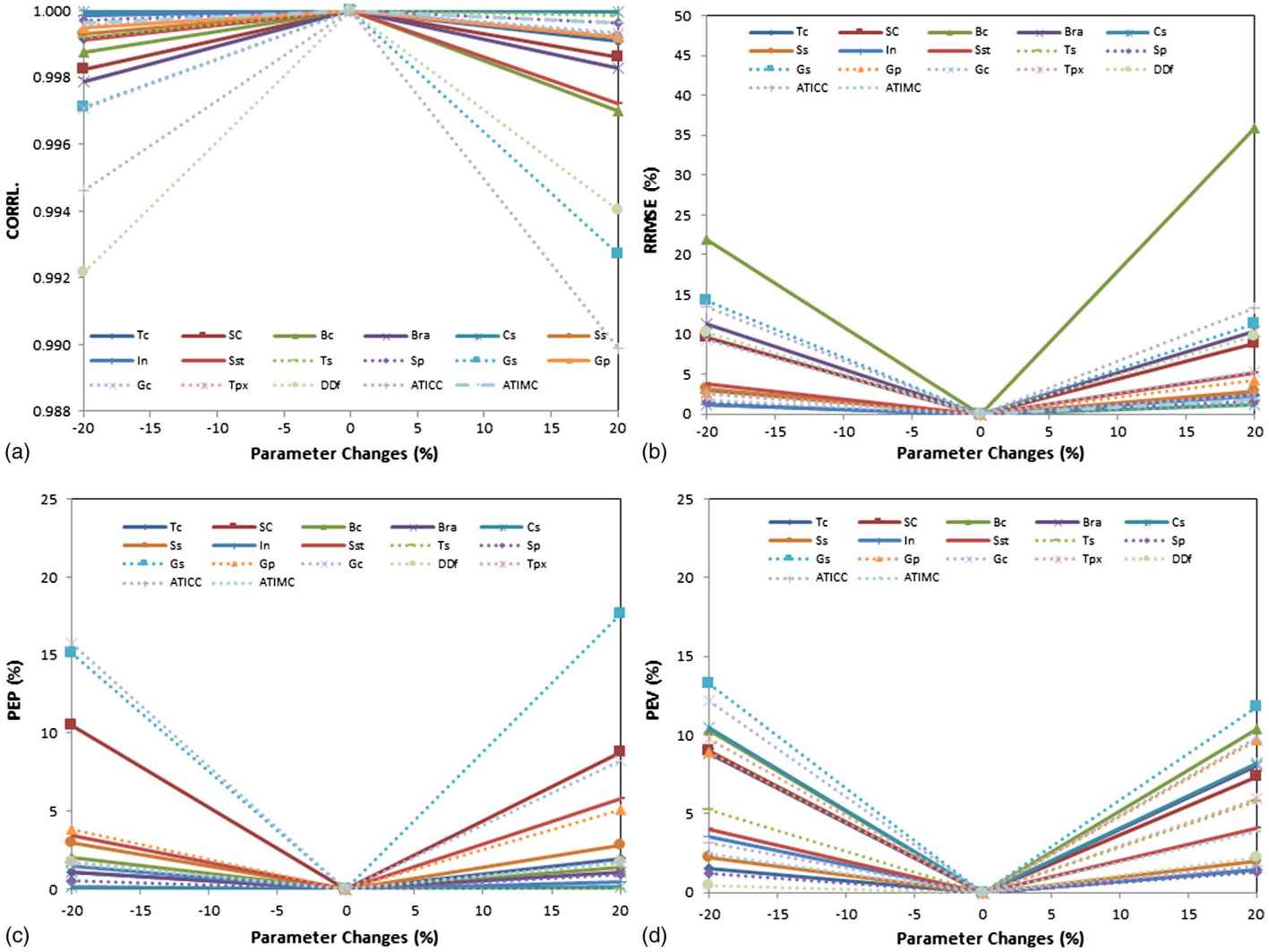

Fig. 7. (a) Sensitivity analysis fitness factors of CORRL; (b) RRMSE; (c) PEP; (d) PEV at Pay-e-Pol hydrometric station

Table 7. Most Sensitive Parameter in Each Sub-Basin

	CORRL		RRMSE		PEP		PEV	
Sub-basin	Parameter	Value	Parameter	Value	Parameter	Value	Parameter	Value
Ghurbaghestan	In	0.985	Bc	65.5	Gs	22.4	Gs	16.2
Pol-e-Chehr	DDF	0.885	ATICC	68.0	Gc	30.4	Gp	21.6
Holeylan	DDF	0.956	Bc	49.8	Gs	26.0	Gs	18.2
Tang-e-Sazbon	ATICC	0.979	Bc	38.2	Gs	20.8	Gs	15.4
Pol-e-Dokhtar	ATICC	0.990	Bc	35.8	Bc	12.4	Gc	18.2
Jelogir	ATICC	0.990	Bc	36.3	Gs	17.4	Gs	13.5
Pay-e-Pol	ATICC	0.990	Bc	35.9	Gs	17.6	Gs	13.3

(e.g., *Gc* or *Gs*) because of the storage they can provide before runoff is generated [Figs. 7(c and d)].

Table 7 summarizes the sensitivity analysis results of the most sensitive parameters across all sub-basins. The results are fairly consistent, illustrating low spatial variability of parameter sensitivity. DDF and ATICC affect the error in the timing of runoff, whereas the overall simulation error (RMSE) is most sensitive to *Bc*.*Gs* and *Gc* significantly affect the magnitude of the peak and flow volume.

The model runs provide insights for snowfall and melt characteristics in light of the unavailability of measured snow data for the region. For example, Fig. 8 shows the precipitation, snowfall, and snowmelt data for Gamasiab sub-basin for the period of 1987–2006, illustrating the effect of temperature on snowfall, as well as premature or delayed snowmelt. The winter of 2006–07 was very cold, with temperatures dropping to –20°C, delaying the melt season until the end of March. By contrast, the warm winter of 1995–96 caused an early onset of snowmelt. Interesting results from a 20-year simulation of the snowmelt model are summarized in Table 8. On average, the share of snowfall from total precipitation or snow coefficient in the KRB varies from 5 to 60%. Gamasiab sub-basin, with an average snow coefficient of 30%, is the

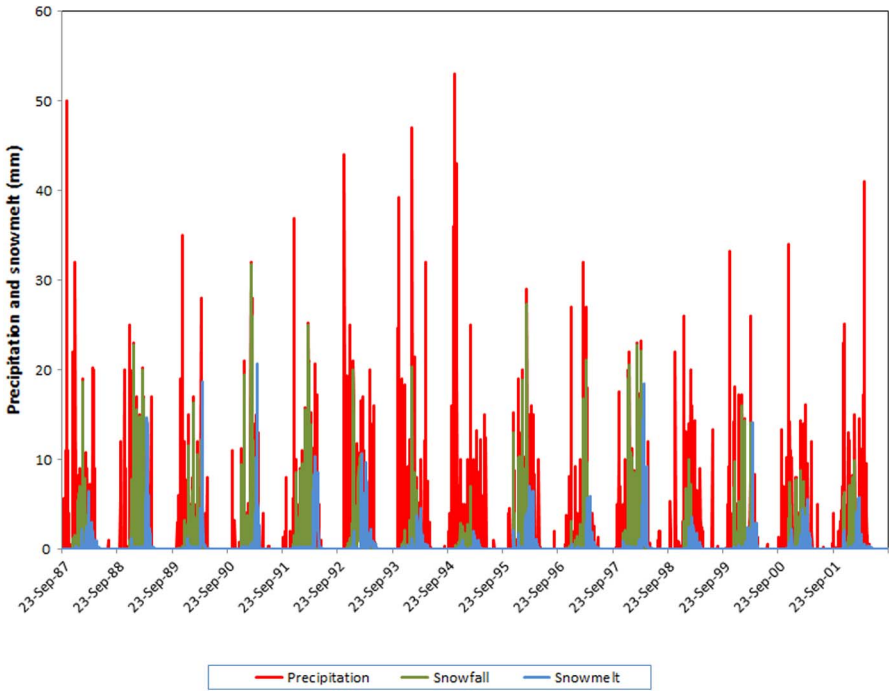

Fig. 8. Comparison of temperature precipitation, snow, and snowmelt for Gamasiab sub-basin during the period of 1987–2006

Table 8. Snow Properties in the KRB Sub-Basins

Sub-basin name	Snowfall (mm)	Snow coefficient range (%)	Snow coefficient average (%)
Gamasiab	138	5–60	33
Gharesu	108	5–48	25
Kashkan	71	5–33	14
Seymareh	120	6–50	24

snowiest part of the basin. The results also show that, on average, the KRB snowfall starts in mid-fall (November) and the snowmelt continues until early summer (July).

Conclusions

Hydrologic models are practical tools that inform water resource planning and management. A good example is the HEC-HMS, a free hydrologic simulation tool that is widely used around the world because of its relatively simple and well-documented conceptual model and its capability to represent different components of the hydrologic cycle. Large river basins with heterogeneous hydroclimatic conditions are typically simulated using continuous hydrologic modeling, spanning a long period with many dry and wet spells. The multitude and diversity of the biophysical parameters governing the precipitation-runoff processes in such basins can turn the manual calibration of HEC-HMS models into a tedious, and at times overwhelming, task. Nonetheless, manual calibration is routinely used because automated calibration, an alternative to manual calibration, may yield physically unrealistic parameter estimates. Using the Karkheh River Basin in western Iran as an HEC-HMS modeling case study, parameter estimation procedures were discussed to improve process-based understanding of large, data-poor, hydroclimatically varied basins. An event-based calibration technique was applied as a practical strategy to facilitate the manual calibration of the CHM, decreasing the calibration time. The presented calibration strategy is based on identifying key hydrological or meteorological parameters and conducting precalibration sensitivity tests on classified calibration period events (e.g., early fall, spring, and winter events) to obtain a better initial estimate of parameter values. It is shown that this additional initial parameter estimation stage significantly improved the modeling performance in terms of goodness-of-fit metrics. As indicated by the split-samplevalidation and fitness factors, parameters of the soil moisture accounting model were adequately calibrated to reproduce daily streamflow for five main sub-basins located upstream of the Karkheh Dam. In general, the model underperformed when simulating low flows, most likely due to uncertainty in the flow naturalization procedure, which accounts for the agricultural return flow in the upper basin. Further, the sensitivity analysis of 17 calibration parameters indicated that hydrograph shape and magnitude of the peak flow were most sensitive to antecedent temperature index cold rate coefficient and baseflow recession coefficient, respectively.

Acknowledgments

The authors acknowledge the Hydro-Environmental and Energy Systems Analysis (HEESA) Research Group members, Carlos Fernández Martín at University of Cantabria for running HEC-HMS during model calibration, and Kondwani Msowoya at University of Central Florida and Felicity Miller at The Way CTU for reviewing an earlier version of this paper.

References

Abbasinejad, A., Afrous, A., and Hedayat, N. (2014). "An artificial neural network approach for predicting floodplain." *Bull. Environ. Pharmacol. Life Sci.*, 3(4), 99–102.

Ahmad, M. D., and Giordano, M. (2010). "The Karkheh River basin: The food basket of Iran under pressure." *Water Int.*, 35(5), 522–544.

Alijani, B. (1995). *Iran climate*, Payame-e-Noor Press, Tehran, Iran.

Ashraf Vaghefi, S., Mousavi, S. J., Abbaspour, K. C., Srinivasan, R., and Yang, H. (2014). "Analyses of the impact of climate change on water

resources components, drought and wheat yield in semiarid regions: Karkheh River basin in Iran." *Hydrol. Process*, 28(4), 2018–2032.
Bennett, T. (1998). "Development and application of a continuous soil moisture accounting algorithm for the Hydrologic engineering center hydrologic modeling system (HEC-HMS)." M.S. thesis, Dept. of Civil and Environmental Engineering, Univ. of California, Davis, CA.
Beven, K. (2016). "Facets of uncertainty: Epistemic uncertainty, non-stationarity, likelihood, hypothesis testing, and communication." *Hydrol. Sci. J.*, 61(9), 1652–1665.
Beven, K, and Westerberg, I. (2011). "On red herrings and real herrings: Disinformation and information in hydrological inference." *Hydrol. Processes*, 25(10), 1676–1680.
Chu, X., and Steinman, A. (2009). "Event and continuous hydrologic modeling with HEC-HMS." *J. Irrig. Drain. Eng.*, 10.1061/(ASCE)0733-9437(2009)135:1(119), 119–124.
Croley, T. E., He, C., and Lee, D. H. (2005). "Distributed-parameter large basin runoff model. II: Application." *J. Hydrol. Eng.*, 10.1061/(ASCE)1084-0699(2005)10:3(182), 182–191.
Cunderlik, J. (2003). "Hydrologic model selection." *CFCAS Project Rep. I*, Dept. of Civil and Environmental Engineering, Univ. of Western Ontario, London, ON, Canada.
Cunderlik, J., and Simonovic, S. P. (2004a). "Selection of calibration and verification data for the HEC-HMS hydrologic model." *CFCAS Project Rep. II*, Dept. of Civil and Environmental Engineering, Univ. of Western Ontario, London, ON, Canada.
Cunderlik, J., and Simonovic, S. P. (2004b). "Calibration, verification, and sensitivity analysis of the HEC-HMS hydrologic model." *CFCAS Project Rep. IV*, Dept. of Civil and Environmental Engineering, Univ. of Western Ontario, London, ON, Canada.
FAO (Food and Agriculture Organization). (1986). *Irrigation water management: Irrigation water needs, training manual no. 3*, FAO Publication, Rome.
FAO (Food and Agriculture Organization). (2004). *Crop evapotranspiration—Guidelines for computing crop water requirements—FAO Irrigation and drainage paper 56*, FAO Publication, Rome.
Ferner, S., and Wigham, J. (1985). "A comparison of melt rate method used in forecasting runoff from an Alberta mountain environment." *53rd Annual Western Snow Conf.*, Brush Prairie, WA, 779–785.
Fleming, M., and Neary, V. (2004). "Continuous hydrologic modeling study with the hydrologic modeling system." *J. Hydrol. Eng.*, 10.1061/(ASCE)1084-0699(2004)9:3(175), 175–183.
Fortin, J. P., Turcotte, R., Massicotte, S., Moussa, R., Fitzback, J., and Villeneuve, J. P. (2001). "Distributed watershed model compatible with remote sensing and GIS data. I: Description of model." *J. Hydrol. Eng.*, 10.1061/(ASCE)1084-0699(2001)6:2(91), 91–99.
Fuladipanah, M., and Jorabloo, M. (2012). "The estimation of snowmelt runoff using SRM case study (Gharasoo basin, Iran)." *World Appl. Sci. J.*, 17(4), 433–438.
Garcia, A., Sainz, A., Revilla, J. A., Alvarez, C., Juanes, J. A., and Puente, A. (2008). "Surface water resources assessment in scarcely gauged basins in the north of Spain." *J. Hydrol.*, 356(3–4), 312–326.
Ghanbarpour, M. R., Saghafian, B., Saravi, M. M., and Abbaspour, K. (2007). "Evaluation of spatial and temporal variability of snow cover in a large mountainous basin in Iran." *Hydrol. Res.*, 38(1), 45–58.
Gyawali, R., and Watkins, D. W. (2013). "Continuous hydrologic modeling of snow-affected watersheds in the Great Lakes basin using HEC-HMS." *J. Hydrol. Eng.*, 10.1061/(ASCE)HE.1943-5584.0000591, 29–39.
Haan, C. T. (2002). *Statistical method in hydrology*, 2nd Ed., Iowa Stat Press, IA.
Hengl, T., Toomanian, N., Reuter, H. I., and Malakouti, M. J. (2007). "Methods to interpolate soil categorical variables from profile observations: Lessons from Iran." *Geoderma*, 140(4), 417–427.
Hock, R. (2003). "Temperature index melt modelling in mountain areas." *J. Hydrol.*, 282(1–4), 104–115.
IRME (Iran Ministry of Energy). (2012). "Karkheh River basin water comprehensive study-second study." Tehran, Iran.
IRMJA (Iran Ministry of Jihad-Agriculture) and (IRMO) Meteorological Organization. (1999). "Iran national documents of irrigation." Tehran, Iran.
IWRM (Iran Water Resources Management). (2009). "Karkheh river basin integrated surface water survey-second study." Tehran, Iran.
Jamali, S., Abrishamchi, A., Madani, K. (2013). "Climate change and hydropower planning in the Middle East: Implications for Iran's Karkheh hydropower systems." *J. Energy Eng.*, 10.1061/(ASCE)EY.1943-7897.0000115, 153–160.
Khatami, S., and Khazaei, B. (2014). "Benefits of GIS application in hydrological modeling: A brief summary." *J. Water Manage. Res.*, 70(1), 41–50.
Klemeš, V. (1986). "Operational testing of hydrological simulation models." *Hydrol. Sci. J.*, 31(1), 13–24.
Leavesley, G. H. (1989). "Problems of snowmelt runoff modelling for a variety of physiographic and climatic conditions." *Hydrol. Sci. J.*, 34(6), 617–634.
Leavesley, G. H., Lichty, R. W., Troutman, B. M., and Saindon, L. G. (1983). "Precipitation-runoff modeling system: User's manual." United States Dept. of the Interior, Geological Survey, Denver.
Maneta, M. P., Pasternack, G. B., Wallender, W. W., Jetten, V., and Schnabel, S. (2007). "Temporal instability of parameters in an event-based distributed hydrologic model applied to a small semiarid catchment." *J. Hydrol.*, 341(3), 207–221.
Martinec, J. (1960). *The degree day factor for snowmelt runoff forecasting*, IAHS Publication, Paris, 468–477.
Martinec, J. (1975). "Snowmelt-runoff model for streamflow forecasts." *Hydrol. Res.*, 6(3), 145–154.
Masih, I. (2011). "Understanding hydrological variability for improved water management in the semi-arid Karkheh basin, Iran." Ph.D. dissertation, Delft Univ. of Technology, Delft, Netherlands.
Masih, I., Uhlenbrook, S., Maskey, S., and Ahmad, M. D. (2010). "Regionalization of a conceptual rainfall-runoff model based on similarity of the flow duration curve: A case study from the semi-arid Karkheh basin, Iran." *J. Hydrol.*, 391(1–2), 188–201.
McCuen, R. H. (1973). "The role of sensitivity analysis in hydrologic modeling." *J. Hydrol.*, 18(1), 37–53.
McEnroe, B. M. (2010). "Guidelines for continuous simulation of streamflow in Johnson County, Kansas, with HEC-HMS." *Technical Rep. to Johnson County Public Works and Infrastructure Stormwater Management Program*, Dept. of Civil, Environmental and Architectural Engineering, Univ. of Kansas, Lawrence, KS.
Morid, S., Gosain, A. K., and Keshari, A. K. (2004). "Response of different snowmelt algorithms to synthesized climatic data for runoff simulation." *J. Earth Space Phys.*, 30(1), 1–9.
Naik, P. K., and Jay, D. A. (2005). "Estimation of Columbia River virgin flow: 1879 to 1928." *Hydrol. Process*, 19(9), 1807–1824.
Neary, V. S., Habib, E., and Fleming, M. (2004). "Hydrologic modeling with NEXRAD precipitation in middle Tennessee." *J. Hydrol. Eng.*, 10.1061/(ASCE)1084-0699(2004)9:5(339), 339–349.
Omani, N., Tajrishy, M., and Abrishamchi, A. (2007). "Modeling of a river basin using SWAT Model and GIS." *Proc., 2nd Int. Conf. on Managing Rivers in the 21st Century: Solutions towards sustainable river basins*, Univ. of Science, Penang, Malaysia, 510–517.
Pirmoradian, N., Kamgar-Haghighi, A. A., and Sepaskhah, A. R. (2004). "Lateral seepage, deep percolation, runoff, and the efficiencies of water use and application in irrigation rice in Kooshkak region in Fars Province, I. R. Iran." *Iran Agric. Res.*, 23–24(2), 1–8.
Saghafian, B., and Davtalab, R. (2007). "Mapping snow characteristics based on snow observation probability." *Int. J. Climatol.*, 27(10), 1277–1286.
Saghafian, B., Davtalab, R., and Kafayati, M. (2016). "Comparison of methods for determining the snowfall threshold temperature and potential area affected by snowfall in the Karkheh, Dez, Karoon and Maroon river basins." *Iran Water Res.*, 10(1), 31–39.
Saxton, K. E., Rawls, W. J., Romberger, S. J., and Papendick, R. I. (1986). "Estimating generalized soil-water characteristics from texture." *Soil Sci. Soc. Am. J.*, 50(4), 1031–1036.

Solaymani, H. R., and Gosain, A. K. (2012). "SWAT application for snow bound Karkheh River basin of Iran." *Proc., 2012 Int. SWAT Conf.*, Indian Institute of Technology, Delhi, India, 334–346.

USACE (U.S. Army Corps of Engineers). (2000). "Hydrologic modeling system HEC-HMS technical reference manual." *Rep. CPD-74A*, Hanover, NH.

USACE (U.S. Army Corps of Engineers). (2010). "Hydrologic modeling system HEC-HMS user's manual." *Rep. CPD-74A*, Hanover, NH.

USDA (U.S. Department of Agriculture). (2004). "Part 630 hydrology national engineering handbook." *Snowmelt*, U.S. Government Printing Office, Washington, DC.

Van Griensven, A., Meixner, T., Grunwald, S., Bishop, T., Diluzio, M., and Srinivasan, R. (2006). "A global sensitivity analysis tool for the parameters of multi-variable catchment models." *J. Hydrol.*, 324(1), 10–23.

Viessman, W. J., and Lewis, G. L. (1995). *Introduction to hydrology*, Addison Wesley Longman, Boston.

Wurbs, R. A. (2006). "Methods for developing naturalized monthly flows at gaged and ungaged sites." *J. Hydrol. Eng.*, 10.1061/(ASCE)1084-0699(2006)11:1(55), 55–64.

Yilmaz, A. G., Imteaz, M. A., and Ogwuda, O. (2012). "Accuracy of HEC-HMS and IBRM models in simulating snow runoffs in upper Euphrates basin." *J. Hydrol. Eng.*, 10.1061/(ASCE)HE.1943-5584.0000442, 342–347.

Zakermoshfegh, M., Ghodsian, M., Salehi Neishabouri, S. A. A., Shakiba, M. (2008). "River flow forecasting using neural network and auto-calibrated NAM model with shuffled complex evolution." *J. Appl. Sci.*, 8(8), 1487–1494.

Zeinivand, H., and De Smedt, F. (2009). "Hydrological modeling of snow accumulation and melting on river basin scale." *Water Resour. Manage.*, 23(11), 2271–2287.